Kinetic Determination of the Fast Exchanging Substrate Water Molecule in the S_3 State of Photosystem II[†,‡]

Warwick Hillier,*[,§] Johannes Messinger,[||] and Tom Wydrzynski[†,§]

Research School of Biological Sciences, The Australian National University, Canberra, ACT 0200, Australia, and Physical Biosciences Division, Lawrence Berkeley National Laboratory, Berkeley, California 94720

Received April 3, 1998; Revised Manuscript Received September 8, 1998

ABSTRACT: In a previous communication we showed from rapid isotopic exchange measurements that the exchangeability of the substrate water at the water oxidation catalytic site in the S_3 state undergoes biphasic kinetics although the fast phase could not be fully resolved at that time [Messinger, J., Badger, M., and Wydrzynski, T. (1995) *Proc. Natl. Acad. Sci. U.S.A. 92*, 3209−3213]. We have since improved the time resolution for these measurements by a further factor of 3 and report here the first detailed kinetics for the fast phase of exchange. First-order exchange kinetics were determined from mass spectrometric measurements of photogenerated O_2 as a function of time after injection of $H_2{}^{18}O$ into spinach thylakoid samples preset in the S_3 state at 10 °C. For measurements made at $m/e = 34$ (i.e., for the mixed labeled $^{16,18}O_2$ product), the two kinetic components are observed: a slow component with $k_1 = 2.2 \pm 0.1$ s^{-1} ($t_{1/2} \sim 315$ ms) and a fast component with $k_2 = 38 \pm 4$ s^{-1} ($t_{1/2} \sim 18$ ms). When the isotopic exchange is measured at $m/e = 36$ (i.e., for the double labeled $^{18,18}O_2$ product), only the slow component (k_1) is observed, clearly indicating that the substrate water undergoing slow isotopic exchange provides the rate-limiting step in the formation of the double labeled $^{18,18}O_2$ product. When the isotopic exchange is measured as a function of temperature, the two kinetic components reveal different temperature dependencies in which k_1 increases by a factor of 10 over the range 0−20 °C while k_2 increases by only a factor of 3. Assuming simple Arrhenius behavior, the activation energies are estimated to be 78 ± 10 kJ mol^{-1} for the slow component and 39 ± 5 kJ mol^{-1} for the fast component. The different kinetic components in the ^{18}O isotopic exchange provide firm evidence that the two substrate water molecules undergo separate exchange processes at two different chemical sites in the S_3 state, prior to the O_2 release step ($t_{1/2} \sim 1$ ms at 20 °C). The results are discussed in terms of how the substrate water may be bound at two separate metal sites.

One of the most important processes in nature is the photosynthetic oxidation of water to molecular oxygen by the chlorophyll/protein complex photosystem II (PSII).[1] The catalytic site for water oxidation involves a cluster of 4 Mn ions and a redox active tyrosine (Y_Z) in a domain called the water oxidizing complex (WOC) (*1, 2*). A fundamental property of the WOC is that O_2 is released with a periodicity of four upon illumination with single turnover light flashes (*3*). To explain this behavior, Kok and co-workers (*4*) proposed that the reaction cycles through five so-called S_n states (for $n = 0, 1, 2, 3, 4$). Beginning in S_0 and traversing to S_4, each S state is advanced by a single quantum event at the photochemical reaction center. Upon reaching the S_4 state, O_2 is released (within 1−2 ms) and the S_0 state is regenerated to begin the cycle again. To account for the observed damping in the period four oscillations, a miss parameter (α) and a double hit parameter (β) were introduced to allow for the mixing of the S_n state populations during a flash sequence. Since the peak O_2 yield occurs on the third flash in dark-adapted samples, the S_1 state was concluded to be dark-stable.

In the original Kok hypothesis it was implied that the two substrate water molecules entered the reaction sequence during the last step, just prior to O_2 release (*4*). More modern models invoke substrate water binding to the WOC at the beginning of the S state cycle (*5, 6*) with the possible involvement of a peroxyl intermediate in the S_3 state (*7*). However, definitive experimental evidence to show how and at which step the O−O bond is formed has remained elusive.

Upon the discovery of a low-temperature, multiline EPR signal that is associated with the S_2 state and arises from the catalytic manganese cluster (*8*), many attempts were made to identify manganese−water interactions through the use of isotopically labeled substrate analogues (e.g., $H_2{}^{17}O$, D_2O, $^{15}NH_3$) (*9*−*14*). Although it is generally concluded from these studies that substrate water is indeed bound to the catalytic Mn in the S_2 state, some of the experimental

* To whom correspondence should be addressed: Hillier@RSBS.ANU.EDU.AU, Tom@RSBS.ANU.EDU.AU.

[†] This work was supported in part by a postdoctoral fellowship from the Australian Research Council and by a grant from the Deutsche Forschungsgemeinschaft (Me 1629/1−1) to J. M.

[‡] Some of the results from this work were presented at the Symposium in Honor of Ken Sauer and Mel Klein held at the University of California, Berkeley, CA, January 7−8, 1998.

[§] The Australian National University.

[||] Lawrence Berkeley National Laboratory.

[1] Abbreviations: EPR, electron paramagnetic resonance; PSII, photosystem II; S_n, redox states of the water oxidizing complex with $n = 0, 1, 2, 3, 4$; WOC, water oxidizing complex.

10.1021/bi980756z CCC: $15.00
Published on Web 11/11/1998

evidence is not easily justified (*15*−*19*). One difficulty in this experimental approach is to unequivocally discriminate between the isotopic exchange by the substrate water and the possible isotopic exchange by other water, oxygen, or proton ligands that may be in the first coordination sphere of the catalytic Mn. Furthermore, there is not yet complete agreement in the literature as to the origin of the S_2 state EPR signals, whether they arise from magnetic couplings between two (*20*) or four (*2*) Mn ions. If the EPR signals arise from only part of the catalytic Mn cluster, then perhaps only part of the manganese−water interactions will be observable.

In another approach to study the binding interactions between the substrate water and the catalytic site, isotopic exchange measurements can be made of photogenerated O_2 upon incubation of a sample in ^{18}O-labeled water using mass spectrometric techniques (*21*−*24*). In the first studies using this approach, it was concluded that there was no nonexchangeable water bound to the WOC prior to the S_4 state (*21*, *22*). However, in these studies an "open" sample chamber system had to be used in which the long mixing and instrument stabilization times needed upon the addition of isotopically labeled water to the sample limited the kinetic resolution of the measurements to ≥30 s. Recently, we were able to reduce the mixing/stabilization times considerably, by a factor of about 1000, through the use of a "closed" chamber system. In the first report of our findings, we showed that the WOC in the S_3 state exhibits two distinct kinetic phases in the ^{18}O isotopic exchange, a slow component with a rate constant of 2.2 s^{-1} at 10 °C and an unresolved fast component (*24*). We have since been able to improve the mixing/stabilization times of our experimental setup by another factor of 3, and we report in this communication the first detailed kinetics for the fast exchanging component.

MATERIALS AND METHODS

Thylakoid membranes were prepared by standard procedures from hydroponically grown spinach and suspended in a medium containing 50 mM HEPES/NaOH (pH 6.8), 400 mM sucrose, 15 mM NaCl, and 5 mM $MgCl_2$. The samples were then frozen as small beads in liquid N_2 and stored at −70 °C. After thawing the thylakoids at room temperature in the dark, they were given a preflash and a 10 min dark period in order to enrich the S_1 population and then kept on ice until measurement. The thylakoid suspension medium was pH calibrated at each temperature used in the various measurements.

The flash-induced O_2 produced by the sample was measured at $m/e = 34$ and $= 36$ with an in-line mass spectrometer (Vacuum Generation MM6, Winsford, UK) for the single and double ^{18}O-labeled O_2, respectively. A closed, stirred cuvette similar to the one used in our earlier work (*24*) but with a smaller internal volume (160 μL) was connected to the mass spectrometer via a dry ice/ethanol bath. A silicon membrane was used to separate the liquid phase from the mass spectrometer inlet, to allow for the passage of gases. Rapid injection of $H_2{}^{18}O$ was achieved with a Hamilton CR-200 syringe that was triggered with a computer-actuated solenoid. Samples were illuminated with saturating light flashes (∼8 μs) from a xenon lamp (FX-193 lamp, 4 μF @ 1 kV capacitor, EG & G, Salem MA) which was positioned directly in front of the sample chamber window. A chlorophyll concentration of 0.9 mg mL^{-1} was used for optimal S/N. The flash and injection sequence was controlled via a computer, and accurate timing intervals were established with a digital oscilloscope.

The exact ^{18}O isotopic enrichment in the sample chamber was determined from the ratio of ^{18}O incorporation into CO_2 measured at $m/e = 44$, 46, and 48, that is,

$$44{:}46{:}48 = (1-\epsilon)^2{:}2\epsilon(1-\epsilon){:}\epsilon^2 = 100\% \qquad (1)$$

where ϵ is the ^{18}O% concentration. The typical ^{18}O enrichment value was $\epsilon = 12.0\% \pm 0.25\%$. The $H_2{}^{18}O$ isotopic equilibration with CO_2 is a consequence of the normal hydration/dehydration reactions of CO_2 in the suspension medium.

The ^{18}O isotopic exchange was measured for the S_3 state at 20, 15, 10, 5, and 0 °C. The thylakoids were loaded in the dark, and the cuvette was degassed for 10−12 min. The injection/flash protocol employed to measure the isotopically labeled O_2 is illustrated below where Δt is the time between the $H_2{}^{18}O$ injection and the third flash:

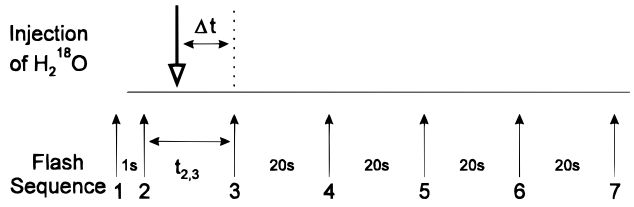

The dark time between the second and third flashes ($t_{2,3}$) was held constant as Δt was varied in order to maintain the same extent of S state deactivation within a data set ($t_{2,3}$ was typically 10 s). Signals from the mass spectrometer were recorded on an $x-t$ plotter. Due to the slow response of the instrument because of the gas diffusion path length, the O_2 yield per flash had to be determined by extrapolating to the time of flash excitation (see Figure 2 in ref *24*). The O_2 background signal caused by the injection of the labeled water (Y_{inj}) was determined by performing separate injections under the same conditions but without flashing. To reduce the size of the Y_{inj}, small quantities of glucose, glucose oxidase, and catalase were added to the labeled water prior to injection. This caused a reproducible reduction in Y_{inj} without interfering with the photogenerated O_2. Typically the Y_{inj} was <3% of the maximum $^{34}Y_3$ (determined at long Δt values measured at $m/e = 34$); however, Y_{inj} was ∼30% of the maximum $^{36}Y_3$ (determined at long Δt values measured at $m/e = 36$) due to a background of atmospheric ^{36}Ar. The measured signal amplitudes for the third flash, $Y_{3(M)}$, less the contributions from the Y_{inj} were normalized to the sum of the flashes 4 → 7 in order to correct for small variations in the sample concentration and changes in the membrane permeability between measurements, that is,

$$Y_{3(N)} = [Y_{3(M)} - Y_{inj}]/\sum_{n=4}^{7} Yn \qquad (2)$$

For comparative purposes the $Y_{3(N)}$ values were then normalized to 1 by dividing by the $Y_{3(N)}$ value at long Δt when the

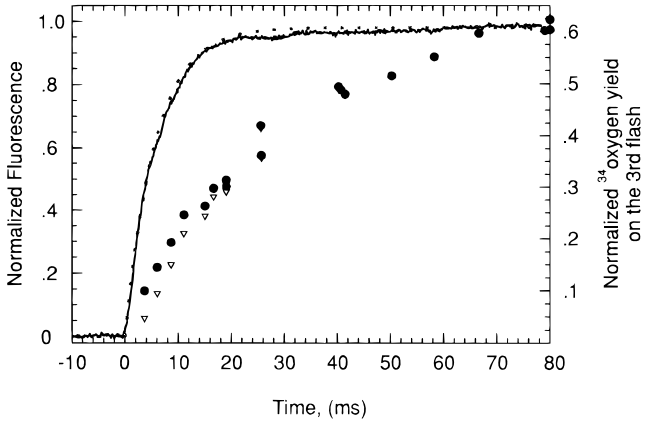

FIGURE 1: Sample chamber injection profile as monitored by fluorescence. The sample chamber contained 160 μL of the standard suspension medium at 10 °C into which 30 μL of a 9% fluorescein solution was injected. The observed fluorescence (solid line) rises to a steady-state level which can be fit to a simple exponential function with $k_{inj} = 175\ s^{-1}$ (dotted line). The O_2 yields measured at $m/e = 34$ after very short isotopic incubation times are plotted before (▽) and after (●) correction of the data for changes in the isotopic enrichment and sample concentration during injection (eq 3, see text for details).

isotopic exchange was complete. Nonlinear curve fitting was performed with Sigma Plot (Jandel Scientific).

To profile the kinetics of the injection and mixing response, fluorescein dye was injected into the sample chamber and the fluorescence yield measured with a PAM 101 fluorimeter (Heinz Waltz, Effeltrich, Germany) modulated at 100 kHz and recorded on a digital oscilloscope. The fluorescence was excited by a LL-450 LED source and detected by an ED-101US/D photodiode (Waltz) through LS-450 and LL-500 (Corion) cutoff filters.

RESULTS

Mass Spectrometric Measurements of Oxygen. The various ^{16}O and ^{18}O isotopic mixtures of dioxygen can be determined by mass spectrometric measurements at $m/e = 32$ for the unlabeled $^{16,16}O_2$, $m/e = 34$ for the mixed labeled $^{16,18}O_2$, and $m/e = 36$ for the double labeled $^{18,18}O_2$. Without additional ^{18}O enrichment, the $^{16,18}O_2$ and $^{18,18}O_2$ background levels are too small to influence our measurements because of the low natural abundance of ^{18}O in water (~0.2%). However, when ^{18}O enrichment is provided, the $^{16,18}O_2$ and $^{18,18}O_2$ produced by spinach thylakoids during a sequence of flashes shows the typical damped, period four oscillation pattern as observed in amperometric measurements (see ref *24*). Kok analysis (*25*) of the mass spectrometric flash patterns measured at 0.05 Hz and 10 °C yielded the following set of parameters: initial S_1 population, $[S_1] = 100\%$; miss parameter, $\alpha = 10\%$; and double hit parameter, $\beta = 4\%$.

To accurately determine the fast ^{18}O exchange kinetics at very short incubation times a correction has to be made for the injection response. Figure 1 shows the injection and mixing profiles of our new sample chamber system as monitored by the fluorescence yield changes upon the injection of fluorescein dye at 10 °C. The fluorescence trace can be fit to a first-order exponential with $k_{inj} = 175\ s^{-1}$ as indicated by the dotted line in Figure 1. There were no significant variations in the fluorescence yield changes due to injection volume (20−40 μL) or to variations in the solution viscosity at different temperatures (data not shown). For these reasons we assume that the mixing in the chamber is instantaneous and that it is due to the force of the injection itself. The normalized $Y_{3(N)}$ values can thus be corrected as follows:

$$Y_{3(C)}(t) = Y_{3(N)}(t)\,\frac{\epsilon}{\epsilon(1 - e^{-175t})(1 + \Delta\text{chl})\,(e^{-175t})} \qquad (3)$$

for

$$\Delta\text{chl} = \frac{[\text{chl}]_{(t=0)} - [\text{chl}]_{(t=\infty)}}{[\text{chl}]_{(t=\infty)}}$$

where $Y_{3(C)}(t)$ is the corrected value for the normalized O_2 yield of the third flash, $Y_{3(N)}(t)$, at a particular Δt. Equation 3 corrects the O_2 yield for the changing levels of ^{18}O enrichment and sample concentration in the sample chamber during the injection process. In principle, a further correction for the nonlinear dependence of the $^{16,18}O_2$ yield from the $H_2{}^{18}O$ enrichment according to eq 1 would apply. This correction, however, is too small under our conditions to affect the data and was consequently ignored. Figure 1 compares the uncorrected $Y_{3(N)}$ values (▽) with the corrected $Y_{3(C)}$ values (●) for the fast phase of exchange measured at $m/e = 34$ in spinach thylakoids at 10 °C. It is obvious that the correction becomes important for data points at $\Delta t \leq 20$ ms. This correction was thus made to all $m/e = 34$ data points at short incubation times but was not performed with the $m/e = 36$ data due to the much slower kinetics (see below), in this case $Y_{3(C)} = Y_{3(N)}$.

^{18}O Exchange in the S_3 State. The kinetics for the ^{18}O isotopic exchange at the water oxidation catalytic site in the S_3 state was measured according to the flash protocol described in the Materials and Methods section. The results are shown in Figure 2, where the corrected O_2 yields of the third flash ($Y_{3(C)}$) are plotted as a function of Δt for the mixed labeled $^{16,18}O_2$ at $m/e = 34$ (top) and for the double labeled $^{18,18}O_2$ at $m/e = 36$ (bottom) at 20, 15, 10, 5, and 0 °C. As the temperature is lowered, the kinetics become slower; hence the time axes in Figure 2 are adjusted accordingly.

The plots of the $m/e = 36$ data exhibit only a single kinetic phase and are best fit with a first-order exponential function, that is,

$$^{36}Y_{3(C)} = (1 - e^{-36kt}) \qquad (4)$$

In contrast, the plots of the $m/e = 34$ data clearly exhibit biphasic kinetics, with distinct fast and slow components. The insets to the top panels in Figure 2 show an expanded time ordinate to reveal the fast phase. As the apparent kinetics for the two components differ by a factor of about 10, the fast phase is virtually complete before the slow phase begins. At short Δt values it is apparent that only one substrate water molecule must be undergoing ^{18}O exchange since there is no fast phase in the $m/e = 36$ data for the double labeled $^{18,18}O_2$. Thus, with an ^{18}O enrichment of $\epsilon = 12\%$, the $m/e = 32{:}34{:}36$ distribution at the short Δt will be 88:12:0. On the other hand, at longer Δt when the second substrate water molecule undergoes ^{18}O exchange, the equilibrium distribution will be 77.44:21.12:1.44 (eq 1).

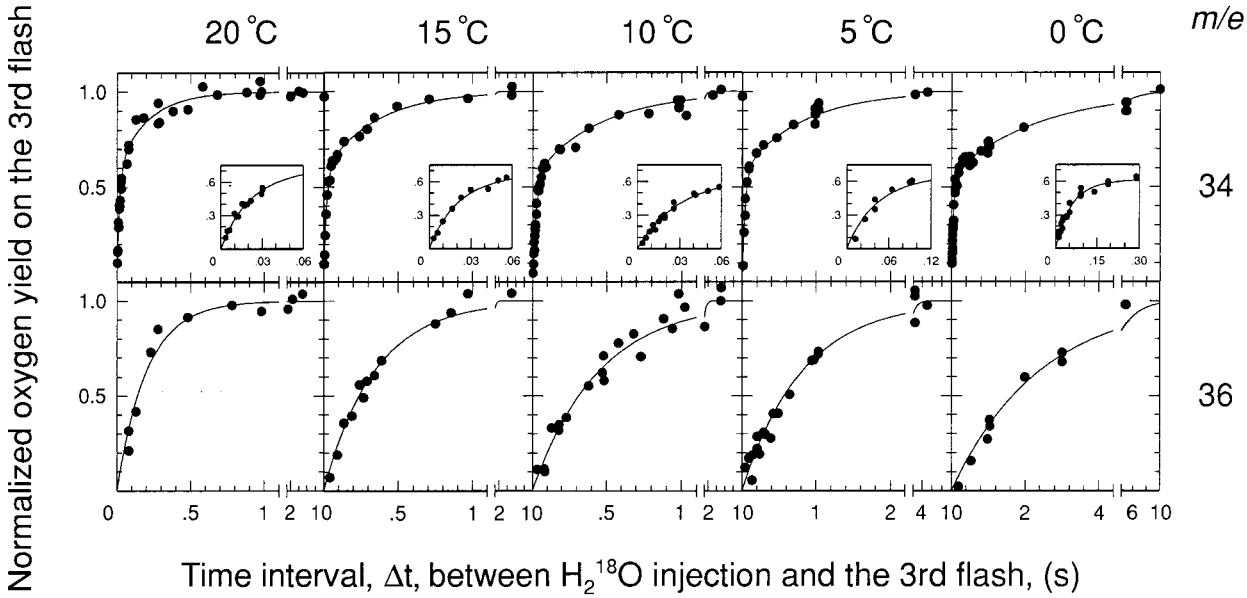

FIGURE 2: The normalized yields of O_2 produced on the third flash by spinach thylakoid samples plotted as a function of $H_2{}^{18}O$ incubation time, Δt, in the S_3 state. Measurements were made at $m/e = 34$ (top) for the mixed labeled $^{16,18}O_2$ and at $m/e = 36$ (bottom) for the double labeled $^{18,18}O_2$ at 20, 15, 10, 5, and 0 °C. The O_2 yields at very short incubation times were corrected for changes in isotopic enrichment and sample concentration during injection (see Figure 1). All measurements were made at 0.9 mg of Chl/mL in an assay medium consisting of 400 mM sucrose, 15 mM NaCl, 5 mM $MgCl_2$, and 50 mM HEPES/NaOH (pH 6.8). Solid lines show first-order kinetic fits according to eqs 4 and 5 (see text for details).

Table 1: Calculated Values for the Slow (k_1) and Fast (k_2) Rates of ^{18}O Exchange in the S_3 State as a Function of Temperature[a]

temp (°C)	k_1 (s^{-1})	k_2 (s^{-1})
20	4.9 ± 0.3	56 ± 6
15	2.9 ± 0.1	54 ± 7
10	2.2 ± 0.1	38 ± 4
5	1.2 ± 0.1	25 ± 7
0	0.42 ± 0.02	19.0 ± 1.2

[a] The kinetic plots are shown in Figure 2.

Therefore, the relative contributions of the fast and slow phases will be unequal, with the fast phase representing ~57% (i.e., 12/21.12) of the total amplitude and the slow phase ~43%. The exchange kinetics for the $m/e = 34$ data can then be exactly fit by the product of two first-order exponential functions as follows:

$$^{36}Y_{3(C)} = 0.57(1 - e^{-^{34}k_2 t}) + 0.43(1 - e^{-^{34}k_1 t}) \quad (5)$$

In this work at all temperatures measured and in our previous work (*24*), we have found through independent analyses that the rate constant for the $m/e = 36$ data (^{36}k) is virtually identical to the rate constant for the slow component in the $m/e = 34$ data ($^{34}k_1$). The obvious explanation is that the water molecule undergoing slow exchange is the rate-limiting step in the formation of the double labeled $^{18,18}O_2$. In analyzing the exchange kinetics, therefore, the data at $m/e = 36$ was cross-correlated with the slow component in the data at $m/e = 34$, using a common rate constant and nonlinear regression (i.e., $^{36}k = {}^{34}k_1$). Table 1 lists the values for the rate constants k_1 and k_2 and their standard errors at various temperatures as derived by this method, using eqs 4 and 5. The fits are shown by the solid lines in Figure 2. It should be kept in mind that the rate constant for the fast component is a lower limit as instantaneous mixing is assumed.

Temperature Dependence of the ^{18}O Exchange Rates. The ^{18}O exchange rate data listed in Table 1 show a significant temperature dependence. Upon increasing the temperature from 0 to 20 °C, k_1 increases by a factor of 10 while k_2 increases by a factor of only about 3. Figure 3 shows Arrhenius plots of k_1 and k_2. In these plots k_2 is practically linear with inverse temperature whereas close inspection of k_1 may reveal a break at around 5 °C. Recently, it has been proposed that the temperature dependence for rate processes occurring within lipid membranes is in fact nonuniform over a broad temperature range and involves a number of change points (*26*). It may be that the apparent break at around 5 °C in k_1 is a change point that is outside of the standard error of the measurements. If this is the case, it is clear that a similar change point does not occur in k_2. Nevertheless, when a simple Arrhenius behavior over the temperature range measured is assumed, linear regression and least-squares analysis of the data yield activation energies of 78 ± 10 kJ

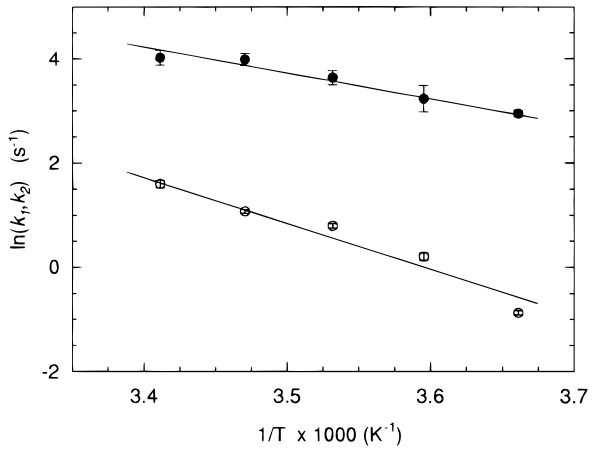

FIGURE 3: Arrhenius plots of the rate constants k_1 (○) and k_2 (●) listed in Table 1, as determined from the kinetic plots of Figure 2. Activation energies were calculated to be 78 ± 10 kJ mol^{-1} for the slow phase of exchange (k_1) and 39 ± 5 kJ mol^{-1} for the fast phase of exchange (k_2) based on the assumtion that the rate constants follow Arrhenius behavior over the temperature range of 0−20 °C.

mol^{-1} for the slow component and 39 ± 5 kJ mol^{-1} for the fast component. These estimates for the activation energies support the idea that the different kinetic components represent different exchange processes.

DISCUSSION

Injection of $H_2{}^{18}O$ into the S_3 state of spinach thylakoid samples and the appearance of ^{18}O in the photogenerated O_2 reflects an isotopic exchange process between the bulk solvent water and the substrate water within the WOC. The data for the mixed labeled $^{16,18}O_2$ product measured at m/e = 34 clearly reveals biphasic kinetics (Figure 2), and in our first work (*24*), we determined that one substrate water molecule must be bound in the S_3 state. However, at the time we could not make any firm conclusions about the second substrate water molecule since, with the kinetic resolution that was available, we could not rule out the possibility that the fast phase of exchange represented a substrate water molecule entering the reaction sequence from the solvent phase during the final S_3 to S_4 to S_0 transition. In the present work, we have improved the time response of our experimental setup (Figure 1) and can now kinetically resolve the fast phase in the ^{18}O isotopic exchange. The rate constants for this component as a function of temperature (Table 1) clearly show that it is kinetically slower than the time needed for O_2 release (*27, 28*) and $Y_Z{}^{ox}$ reduction (*29, 30*) on the final S_3 to S_4 to S_0 transition (i.e., 1−2 ms). Thus, we conclude that both substrate water molecules must be bound in the S_3 state. Since the rate constants and temperature dependencies for the two phases of ^{18}O isotopic exchange are significantly different from each other (Figures 2 and 3, Table 1), we also conclude that the two substrate water molecules must be undergoing separate exhange processes at chemically different sites.

The Slow ^{18}O Isotopic Exchange Process. The exchange process for the substrate water undergoing slow ^{18}O isotopic exchange in the S_3 state has a rate constant of k_1 = 2.2 ± 0.1 s^{-1} at 10 °C (Table 1) and an estimated activation energy of 78 ± 10 kJ mol^{-1} at temperatures above 0 °C (Figure 3). According to our current knowledge, it is likely that the substrate water binds to the metal cofactors of the WOC, that is, either to Mn^{III} or Mn^{IV} ions (*31, 32*) or to a Ca^{II} ion (*33*−*36*). For comparison, Table 2 lists the water ligand exchange rates for various metal complexes. In the first instance, it seems unlikely that the slow exchange process involves a hydrated Ca^{II} ion as the rates of exchange differ by 7−8 orders of magnitude (*37*). However, unfortunately, water ligand exchange rates have not been determined for hydrated Mn^{III} or Mn^{IV} ions as they do not formally exist in aqueous solution. Nevertheless, it may be expected that rates for manganese−water exchange follow the sequence $k_{ex}(Mn^{II}{-}OH_2) > k_{ex}(Mn^{III}{-}OH_2) > k_{ex}(Mn^{IV}{-}OH_2)$, as the ionic radius of the metal center decreases (*38*). On the basis of a comparison with Fe and Ru complexes (*39*−*41*), the water ligand exchange rates for Mn ions may be expected to slow by ∼10^{-4} s^{-1} for each formal oxidation state increase (Table 2). Similarly, a comparison with Cr^{III} (*42*) can provide a clue to the magnitude of the water ligand exchange rate for Mn^{IV} since the two ions are isoelectronic with a stable d^3 configuration (Table 2). In general, therefore, we may expect that the water ligand exchange rates are in the range of 10^{-3} to 10^{-1} s^{-1} for Mn^{III} and 10^{-5} to 10^{-7} s^{-1} for Mn^{IV}.

Table 2: Ligand Exchange Rates for Various Hydrated Metal Complexes

	exchange rate (s^{-1})	reference
S_3 state of PS II		
slow phase (k_1 at 10 °C)	2×10^0	this work
fast phase (k_2 at 10 °C)	4×10^1	work
hydrated M^{2+} ions		
$[Ca(H_2O)_6]^{2+}$ (dimagnetic)	3×10^8	*37*
$[Fe(H_2O)_6]^{2+}$ (high spin)	4×10^6	*39*
$[Ru(H_2O)_6]^{2+}$ (low spin)	2×10^{-2}	*41*
hydrated M^{3+} ions		
$[Fe(H_2O)_6]^{3+}$ (high spin)	2×10^2	*40*
$[Ru(H_2O)_6]^{3+}$ (low spin)	4×10^{-6}	*41*
$[Cr(H_2O)_6]^{3+}$ (high spin)	2×10^{-6}	*42*
terminal oxo ligands		
$[TiO(H_2O)_5]^{2+}$	2×10^4	*43, 44*
$[VO(H_2O)_5]^{2+}$	1×10^{-5}	*45*
μ-oxo bridges		
$[Fe^{III}{}_2]$ − ribonucleotide reductase	8×10^{-4}	*49*
$[Mo^{V}{}_2\ O_4\ (OH_2)_6]^{2-}$	3×10^{-6}	*50*
$[Mo^{IV}{}_3\ O_4\ (OH_2)_9]^{4-}$	$<10^{-8}$	*51*

Clearly though, there are factors other than the redox state of the metal center that could strongly influence water ligand exchange. One of these in particular is the protonation of the bound water ligand. In general, it may be expected that $k_{ex}(M{-}OH_2) > k_{ex}(M{-}OH) > k_{ex}(M{=}O)$, where protonation of the bound water ligand will depend on the pK_a of the metal complex, which in turn is a function of not only the redox state of the metal center but also of the type(s) of other ligands. This behavior is illlustrated in Table 2 by the large difference in the rate constants for oxo ligand exchange in a Ti=O complex (*43, 44*) and in a V=O complex (*45*). In this case, it is believed that the Ti=O complex is very easily protonated (*43*). The importance of protonation is also observed with the horseraddish peroxidase Fe^{IV}=O complex which undergoes ^{18}O exchange at pH 7 but not at pH 9 (*46*). Consequently, although higher oxidation state Mn ions will tend to polarize bound water favoring hydroxyl or oxo ligands, the pK_a of the Mn complex as influenced by the other ligands bound to it could have a strong effect on the water ligand exchange rate. The pK_a's for various Mn complexes have been reported elsewhere (*47*).

It has also been proposed that a bridging di $(Mn)_2$ μ-oxo intermediate may be involved in the water oxidation chemistry (*48*). However, in this case the exchange process should be very slow. As shown in Table 2, the exchange rate for the μ-oxo bridge in ribonucleotide reductase (*49*) and in a $[Mo^{V}{}_2\ O_4(OH_2)_6]^{2+}$ complex (*50*) is $<10^{-6}$ s^{-1} while in a $[Mo^{IV}{}_3O_4(OH_2)_9]^{4+}$ complex (*51*) no exchange was discernible over a 2 year period. Nevertheless, a more labile oxygen bridging structure for the catalytic Mn in the WOC cannot be excluded conclusively at present.

Other important factors that may influence the isotopic exchange at a metal site are the coordination geometry (axial vs equatorial) and whether the metal center is high or low spin. These factors are yet to be defined for the catalytic Mn in the WOC, but it is generally believed that the catalytic Mn is mainly coordinated to carboxyl groups (*48, 52*) which would tend to promote high spin clusters. In summary, our data for the slow isotopic exchange process in the S_3 state of the WOC would be consistent with a terminally bound substrate water ligand most likely in the form of Mn^{III}—OH, or Mn^{IV}—OH.

The Fast ^{18}O Isotopic Exchange Process. The exchange process for the substrate water molecule undergoing the fast ^{18}O exchange in the S_3 state has a rate constant of $k_2 = 38 \pm 4\ s^{-1}$ at 10 °C (Table 1) and an estimated activation energy of 39 ± 5 kJ mol^{-1} at temperatures above 0 °C (Figure 3). Since k_2 differs from k_1 by only about an order of magnitude at all temperatures measured, the second substrate binding site could have a ligand configuration similar to, but nonequivalent with, those proposed above for the first substrate binding site, that is, either Mn^{III}—OH or Mn^{IV}—OH. However, because the difference between k_1 and k_2 is not very large, manganese−substrate pair combinations differing by a formal oxidation state may be considered unlikely, unless countered by significant differences in ligation. Thus, the exchange processes that we measure may reflect substrate binding to terminal sites on two separate Mn ions of the same oxidation state, as has been suggested earlier (*5*, *6*). Our present data, however, gives no information with respect to the suggestion that two partially deprotonated water molecules exist in redox isomerization with a peroxyl intermediate in the S_3 state (*7*).

Regardless of the above arguments, it cannot be absolutely excluded at this time that the fast exchanging component does not represent a diffusional or isotopic equilibration process. Since the catalytic site is located within the protein domain of the WOC, away from the bulk solvent phase, a phenomonological water channel most likely exists and may provide an important role in regulating the water oxidation chemistry (*53*). In this case, solvent $H_2{}^{18}O$ may come into equilibrium with the bound substrate water at the catatlytic site either through mass water movement or via isotopic exchange over an chain of water molecules through the protein matrix. Water channels have recently been proposed for proteins such as cytochrome *c* oxidase (*54*, *55*) and cytochrome P450 (*56*). Although water exchange within small proteins has been determined to be very fast (10^3−$10^9\ s^{-1}$) (*57*, *58*), water movement into the WOC may in particular be functionally restricted. However, in order for such a water channel to have a role in the exchange process, it would have to be assumed that one substrate water molecule binds to a site in more rapid exchange, such as a Ca^{II} ion (*59*), and that the channel does not limit the exhange at the second substrate water binding site.

Although with the present data we cannot determine whether the differences between slow and fast ^{18}O exchange processes in the S_3 state are due to differences in charge delocalization at metal sites, the protonation and hydrogen bonding of the bound substrate water, and/or the structure of the protein matrix surrounding the catatlytic site, we anticipate that measurements of the ^{18}O exchange rates as a function of S states, pH, deuteration, metal substitution, and protein modification will help discern some of these possibilities.

ACKNOWLEDGMENT

The authors gratefully acknowledge Alan Sargeson and Ron Pace for many fruitful discussions and Murray Badger for technical assistance in the use of the mass spectrometer.

REFERENCES

1. Diner, B., and Babcock, G. T. (1996) in *Oxygenic Photosynthsis: The Light Reactions* (Ort, D. R., and Yocum, C. F., Eds.) pp 213−247, Kluwer, Dordrecht, The Netherlands.
2. Britt, D. R. (1996) in *Oxygenic Photosynthesis: The Light Reactions* (Ort, D. R., and Yocum, C. F., Eds.) pp 137−164, Kluwer, Dordrecht, The Netherlands.
3. Joliot, P., Barbieri, G., and Chaband, R. (1969) *Photochem. Photobiol. 10*, 309−329.
4. Kok B., Forbush B., and McGloin, M. (1970) *Photochem. Photobiol. 11*, 457−475.
5. Witt, H. T. (1996) *Ber. Bunsen-Ges. Phys. Chem. 100*, 1923−1942.
6. Hoganson, C. W., and Babcock, G. T. (1997) *Science 277*, 1983−1956.
7. Renger, G. (1997) *Physiol. Plant. 100*, 828−841.
8. Dismukes, G. C., and Siderer, Y. (1981) *Proc. Natl. Acad. Sci. U.S.A. 78*, 274−278.
9. Hansson, Ö., Andréasson, L.-E., and Vänngård, T. (1986) *FEBS Lett. 195*, 151−154.
10. Nugent, J. H. A. (1987) *Biochim. Biophys. Acta 893*, 184−189.
11. Kawamori, A., Inai, T., Ono, T., and Inoue, Y. (1989) *FEBS Lett. 254*, 219−223.
12. Britt, D. R., Zimmermann, J.-L., Sauer, K., and Klein M. P. (1989) *J. Am. Chem. Soc. 111*, 3522−3532.
13. Britt, D. R., Derose, V. J., Yachandra, V. K., Kim, D. H., Sauer, K., and Klein M. P. (1990) in *Current Research in Photosynthesis*, (Baltscheffsky, M., Ed.) Vol. 1, pp 769−772, Kluwer Academic Publishers, The Netherlands.
14. Fiege, R., Zweygart, W., Bittl, R., Adir, N., Renger, G., and Lubitz, W. (1996) *Photosynth. Res. 48*, 227−237.13
15. Yachandra, V. K., Guiles, R. D., Sauer, K., and Klein, M. P. (1986) *Biochim. Biophys. Acta 850*, 333−342.
16. Haddy, A., Aasa, R., and Andréasson L.−E. (1989) *Biochemistry 28*, 6954−6959.
17. Tang, X.-S., Sivaraja, M., and Dismukes, G. C. (1993) *J. Am. Chem. Soc. 115*, 2382−2389.
18. Andréasson, L.-E., Hansson Ö., and von Schenck, K. (1988) *Biochim. Biophys. Acta 936*, 351−360.
19. Turconi, S., MacLachlan, D. J., Bratt, P. J., Nugent, J. H. A., and Evans, M. C. W. (1997) *Biochemistry 36*, 879−885.
20. Smith, P. J., and Pace, R. J. (1996) *Biochim. Biophys. Acta 1275*, 213−220.
21. Radmer, R., and Ollinger, O. (1980) *FEBS Lett. 110*, 57−61.
22. Radmer, R., and Ollinger, O. (1986) *FEBS Lett. 195*, 285−289.
23. Bader, K. P., Thibault, P., and Schmid, G. H. (1987) *Biochim. Biophys. Acta 893*, 564−571.
24. Messinger, J., Badger, M., and Wydrzynski, T. (1995) *Proc. Natl. Acad. Sci. U.S.A.* 92, 3209−3213.
25. Forbrush, B., Kok, B., and McGloin, M. (1971) *Photochem. Photobiol. 14*, 307−321.
26. Jones, R. H., and Day, I. (1995) *Chem. Phys. Lipids 76*, 1−6
27. Jursinic, P., and Dennenburg, R. J. (1990) *Biochim. Biophys. Acta 1020*, 195−206.
28. Lavorel, J. (1992) *Biochim. Biophys. Acta 1101*, 33−40.
29. Babcock, G. T., Blankenship, R. E., and Sauer, K. (1976) *FEBS Lett. 61*, 286−289.
30. Razeghifard, M. R., Klughammer, C., and Pace, R. J. (1997) *Biochemistry 36*, 86−92.
31. Ono, T., Noguchi, T., Inoue, Y., Kusunoki, M., Matsushita, and Oyanagi, H. (1992) *Science 258*, 1335−1337.
32. Roelofs, T. A., Liang, W., Latimer, M. J., Cinco, R. M., Rompel, A., Andrews, J. C., Sauer, K., Yachandra, V. K., and Klein, M. P. (1996) *Proc. Natl. Acad. Sci. U.S.A. 93*, 3335−3340.
33. Ono, T.-A., and Inoue, Y. (1988) *FEBS Lett. 227*, 147−152.
34. Ådelroth, P., Lindberg, K., and Andréasson, L.-E. (1995) *Biochemistry 34*, 9021−9027.
35. Chen, C., Kazimir, J., and Cheniae, G. M. (1995) *Biochemistry 34*, 13511−13526
36. Latimer, M. J., DeRose, V. J., Mukerji, I., Yachandra, V. K., Sauer, K., and Klein, M. P. (1995) *Biochemistry 34*, 10898−10909.
37. Eigen, M. (1963) *Pure Appl. Chem. 6*, 97−115.
38. Lincoln, S. F., and Merbach, A. E. (1995) *Adv. Inorg. Chem. 42*, 1−88

39. Ducommun, Y., Newman K. E., and Merbach, A. E. (1980) *Inorg. Chem. 19,* 3696−3703.
40. Grant, M., and Jordan, R. B. (1981) *Inorg. Chem. 20,* 55−60.
41. Rapaport, I., Helm., L., Merbach, A. E., Berhard, P., and Ludi, A. (1988) *Inorg. Chem. 27,* 873−879.
42. Xu., F.-C., Krouse, H. R., and Swaddle, T., W. (1985) *Inorg. Chem. 24,* 267−270
43. Comba, P., and Merbach, A. (1987) *Inorg. Chem. 26,* 1315−1323.
44. Dellavia, I., Helm, L., and Merbach, A. E. (1992) *Inorg. Chem. 31,* 4151−4154.
45. Johnson, M. D., and Murmann, R. K. (1983) *Inorg. Chem. 22,* 1068−1072.
46. Hashimoto, S., Tatsuno, Y., and Kitagawa, T. (1986) *Proc. Natl. Acad. Sci. U.S.A. 83,* 2417−2421.
47. Tommos, C., and Babcock, G. T. (1998) *Acc. Chem. Res. 31,* 18−25
48. Yachandra, V. K., Sauer, K., and Klein, M. P. (1996) *Chem. Rev. 96,* 2927−2950.
49. Sjöberg, B.-M., Loehr, T. M., and Sanders-Loehr, J. (1982) *Biochemistry 21,* 96−102.
50. Murmann, R. K. (1980) *Inorg. Chem. 19,* 1765−1770.
51. Richens, D. T., Helm, L., Pittet, P.-A., Merbach, A. E., Nicoló, F., and Chapuis, G. (1989) *Inorg. Chem. 28,* 1394−1402.
52. Dittmer, J., and Dau, H. (1997) *Ber. Bunsen-Ges. Phys. Chem. 100,* 1993−1998.
53. Wydrzynski, T., Hillier, W., and Messinger, J. (1996) *Physiol. Plant. 96,* 342−350
54. Iwata, S., Ostermeier, C., Ludwig, B., and Michel, H. (1995) *Nature 376,* 660−669.
55. Tsukihara, T., Aoyama, H., Yamashita, E., Tomizaki, T., Yamaguchi, H., Shinzawa-Itoh, K., Nakashima, R., Yaono, R., and Yoshikawa, S. (1996) *Science 272,* 1136−1144.
56. Opera, T. I., Hummer G., and García, A. E. (1997) *Proc. Natl. Acad. Sci. U.S.A. 94,* 2133−2138.
57. Otting, G., Liepinsh, E., and Wuthrich, K. (1991) *Science 254,* 974−980.
58. Dötsch, V., and Wider, G. (1995) *J. Am. Chem. Soc. 117,* 6064−6070.
59. Rutherford, A. W. (1989) *Trends Biochem. Sci. 14,* 227−232.

BI980756Z